

## Nonsuperatomic $[\text{Au}_{23}(\text{SC}_6\text{H}_{11})_{16}]^-$ Nanocluster Featuring Bipyramidal $\text{Au}_{15}$ Kernel and Trimeric $\text{Au}_3(\text{SR})_4$ Motif

Anindita Das,<sup>†</sup> Tao Li,<sup>‡</sup> Katsuyuki Nobusada,<sup>\*,§,||</sup> Chenjie Zeng,<sup>†</sup> Nathaniel L. Rosi,<sup>‡</sup> and Rongchao Jin<sup>\*,†</sup>

<sup>†</sup>Department of Chemistry, Carnegie Mellon University, Pittsburgh, Pennsylvania 15213, United States

<sup>‡</sup>Department of Chemistry, University of Pittsburgh, Pittsburgh, Pennsylvania 15260, United States

<sup>§</sup>Department of Theoretical and Computational Molecular Science, Institute for Molecular Science, Myodaiji, Okazaki 444-8585, Japan

<sup>||</sup>Elements Strategy Initiative for Catalysts and Batteries (ESICB), Kyoto University Katsura, Kyoto 615-8520, Japan

 Supporting Information

**ABSTRACT:** We report the X-ray structure of a cyclohexanethiolate-capped  $[\text{Au}_{23}(\text{SR})_{16}]^-$  nanocluster (counterion: tetraoctylammonium,  $\text{TOA}^+$ ). The structure comprises a cuboctahedron-based bipyramidal  $\text{Au}_{15}$  kernel, which is protected by two staple-like trimeric  $\text{Au}_3(\text{SR})_4$  motifs, two monomeric  $\text{Au}(\text{SR})_2$  and four plain bridging SR ligands. Electronic structure analysis reveals nonsuperatomic feature of  $[\text{Au}_{23}(\text{SR})_{16}]^-$  and confirms the  $\text{Au}_{15}$  kernel and surface motifs. The  $\text{Au}_{15}$  kernel and trimeric staple motif are unprecedented and offer new insight in understanding the structure evolution of gold nanoclusters.

Atomically precise metal nanoclusters have recently emerged as a new frontier in nanoscience research.<sup>1–13</sup> Gold nanoclusters protected by thiolate ligands (denoted as  $\text{Au}_n(\text{SR})_m$ , where  $n$  and  $m$  represent the numbers of metal atoms and ligands, respectively) are of particular interest due to their extraordinary stability, physicochemical properties, and many promising applications.<sup>14–19</sup> In fundamental research, it is of major importance to understand how the atoms in the nanocluster are packed and how the surface is protected by ligands, as both aspects determine the stability and properties of  $\text{Au}_n(\text{SR})_m$  nanoclusters.<sup>20–27</sup> Although a number of size-discrete nanoclusters have been identified,<sup>1–5,28–36</sup> only a few of them have been structurally characterized by single crystal X-ray crystallography.<sup>20–23,37–39</sup> Herein, we report the synthesis and structure determination of a new  $[\text{Au}_{23}(c\text{-C}_6)_{16}]^-$  nanocluster (counterion:  $\text{TOA}^+$ , and  $c\text{-C}_6$  represents cyclohexanethiolate). On the basis of the crystal structure, we further carried out density functional theory (DFT) analysis of the electronic structure and interpreted the optical spectrum of the cluster.

The synthesis of  $[\text{Au}_{23}(c\text{-C}_6)_{16}]^-$  involved  $\text{NaBH}_4$  reduction of gold salt following a one-phase method using methanol as the solvent<sup>34</sup> and cyclohexanethiol<sup>32</sup> as the ligand (see Supporting Information (SI) for details). After reaction overnight, pure  $[\text{Au}_{23}(c\text{-C}_6)_{16}]^-$  nanoclusters resulted via spontaneous size focusing. Single crystal growth of the nanoclusters was performed via vapor diffusion of pentane into a concentrated solution of the nanoclusters in dichloromethane for 1–2 days.

Single crystal X-ray crystallography revealed the total structure of the nanocluster (Figure 1). The counterion ( $\text{TOA}^+$ ) for the anionic cluster was also found, albeit the carbon chains were heavily disordered. To reveal the details of the structure, we start with the  $\text{Au}_{23}\text{S}_{16}$  framework (Figure 2A).

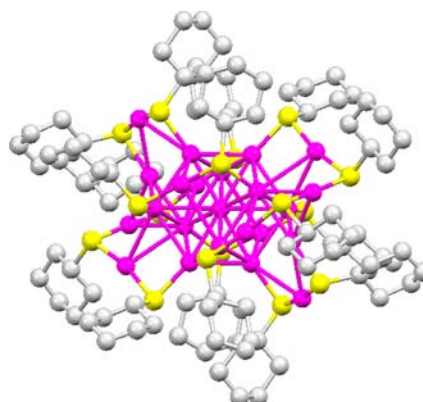


**Figure 1.** Crystal structure of a cyclohexanethiolate-protected  $[\text{Au}_{23}(c\text{-C}_6)_{16}]^-$  nanocluster ( $\text{TOA}^+$  counterion omitted). Color labels: magenta = Au, yellow = S, gray = C; all H atoms not shown.

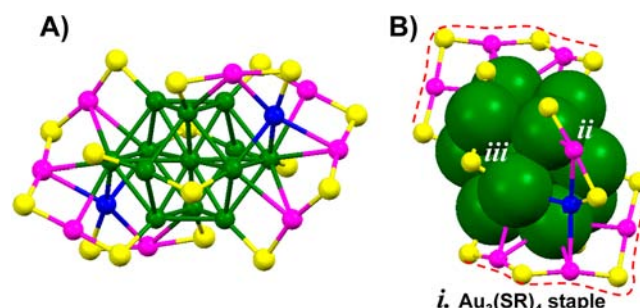


**Figure 2.** (A) The  $\text{Au}_{23}\text{S}_{16}$  framework with the cuboctahedron highlighted in green and the two extra atoms in blue. (B) Thiolate-binding motifs in  $[\text{Au}_{23}(c\text{-C}_6)_{16}]^-$ : (i)  $\text{Au}_3(\text{SR})_4$  staple, (ii)  $\text{Au}(\text{SR})_2$  staple, and (iii) simple thiolate bridging mode. (Color labels: magenta/green/blue = Au, yellow = S).

Received: September 4, 2013

Published: November 25, 2013



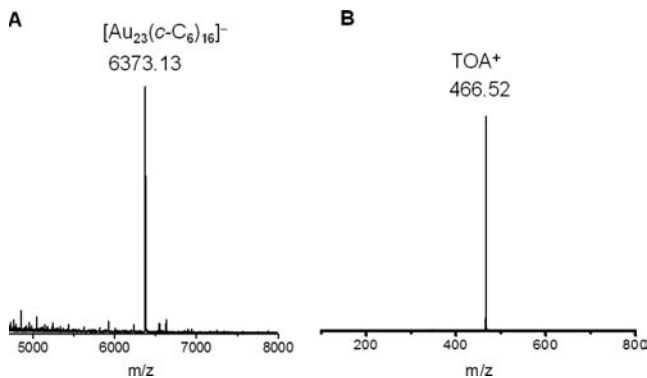


**Figure 3.** ESI-MS analysis of  $[\text{Au}_{23}(\text{c-C}_6)_{16}]^- \cdot \text{TOA}^+$ . (A) Negative mode mass spectrum of  $[\text{Au}_{23}(\text{c-C}_6)_{16}]^-$ . (B) Positive mode spectrum for the counterion  $\text{TOA}^+$ , where  $\text{TOA} = {}^+\text{N}(\text{C}_8\text{H}_{17})_4$ .

An  $\text{Au}_{13}$  cuboctahedron (Figure 2B, highlighted in green) is identified in  $[\text{Au}_{23}(\text{c-C}_6)_{16}]^-$ , which is in contrast with the  $\text{Au}_{13}$  icosahedron in  $[\text{Au}_{25}(\text{SCH}_2\text{CH}_2\text{Ph})_{18}]^q$  ( $q = -1, 0$ ).<sup>21–23</sup> Starting from the center of the cuboctahedron, the radial Au–Au bond lengths give rise to an average of  $2.96 \pm 0.28$  Å, in comparison to the  $2.79 \pm 0.01$  Å in the icosahedral  $\text{Au}_{13}$  of  $[\text{Au}_{25}(\text{SCH}_2\text{CH}_2\text{Ph})_{18}]^q$ .<sup>21–23</sup> The peripheral Au–Au bond lengths of the  $\text{Au}_{13}$  cuboctahedron give an average of  $3.00 \pm 0.27$  Å.

The cuboctahedral kernel is protected by two trimeric  $\text{Au}_3(\text{SR})_4$  staples with one on the top and the other at the bottom (Figure 2B, labeled *i* and highlighted with dashed curves), two monomeric  $\text{Au}(\text{SR})_2$  staples with one in the back and the other in the front (Figure 2B, labeled *ii*), and four simple bridging SR ligands with two in the back and two in the front (Figure 2B, labeled *iii*). Among these surface-protecting

motifs, the trimeric  $\text{Au}_3(\text{SR})_4$  staple is indeed for the first time observed experimentally. Such a trimeric staple was predicted to exist in earlier theoretical works<sup>40,41</sup> in the structure of the experimentally identified  $\text{Au}_{20}(\text{SR})_{16}$ .<sup>42</sup> The theoretical structure of  $\text{Au}_{20}(\text{SR})_{16}$  was predicted to possess a prolate  $\text{Au}_8$  kernel with four trimeric staple motifs.<sup>40,41</sup> Recently,  $\text{Au}_{18}(\text{SR})_{14}$  and  $\text{Au}_{15}(\text{SR})_{13}$  nanoclusters were also predicted to possess trimeric staples.<sup>25,43</sup> The trimer configuration observed in the X-ray structure of  $[\text{Au}_{23}(\text{c-C}_6)_{16}]^-$  is comparable to the theoretically constructed trimer.

We also found two extra surface Au atoms in  $[\text{Au}_{23}(\text{c-C}_6)_{16}]^-$  (Figure 2B, highlighted in blue), each serving as a “hub” for linking to the trimeric and monomeric staples (Figure 2B) with  $\text{Au}_{\text{hub}}-\text{Au}_{\text{staple}}$  distance of  $\sim 2.93$  Å. The  $\text{Au}_{\text{hub}}-\text{Au}_{\text{kernel}}$  distances ( $\sim 2.7$  Å to the underlying kernel’s gold atoms) are even shorter than the average radial Au–Au distance (2.96 Å) in the cuboctahedron, thus these two extra surface Au atoms are more strongly associated with the kernel. The kernel is better described to be a  $\text{Au}_{15}$  bipyramidal (Figure S1), rather than a  $\text{Au}_{13}$  cuboctahedron. This  $\text{Au}_{15}$  kernel is further confirmed by DFT analysis of the electronic property of the cluster. The bipyramidal  $\text{Au}_{15}$  can be viewed as a bicapped cuboctahedron along its four-fold axis.

The cluster formula and charge state were confirmed by electrospray ionization mass spectrometry (ESI-MS) analysis. ESI-MS (negative ion mode) revealed a prominent peak at  $m/z = 6373.13$  (Figure 3A), corresponding to the formula of the intact cluster  $[\text{Au}_{23}(\text{c-C}_6)_{16}]^-$  (calculated formula weight: 6373.16). The  $\text{TOA}^+$  counterion was also found in the positive mode mass spectrum (Figure 3B, expected mass: 466.53, observed: 466.52 Da), confirming the  $-1$  charge of the cluster (note: one  $\text{TOA}^+$  per cluster was found in the crystal structure). The purity of the product was further confirmed

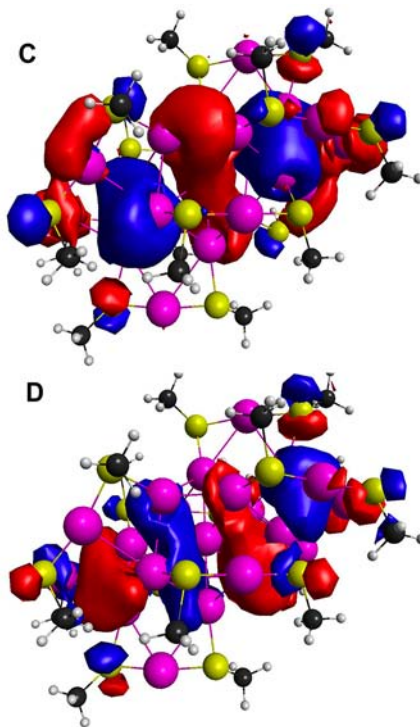
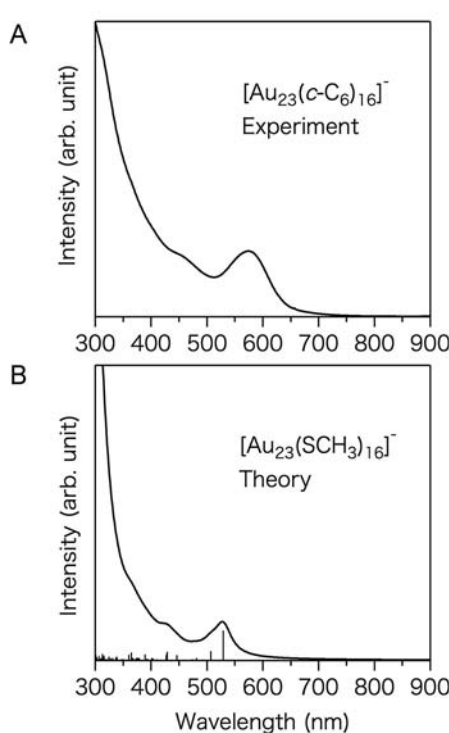


**Figure 4.** (A) Experimental UV–vis spectrum of  $[\text{Au}_{23}(\text{c-C}_6)_{16}]^-$  and (B) theoretically simulated spectrum of the  $[\text{Au}_{23}(\text{SCH}_3)_{16}]^-$  model cluster. (C) Schematic diagram of HOMO of  $[\text{Au}_{23}(\text{SCH}_3)_{16}]^-$  and (D) LUMO of the cluster.

by thermogravimetric analysis, and a 33.8 wt % loss was observed (Figure S2), consistent with the formula (calculated loss: 33.8%).

To gain insight into the newly observed trimeric staple motif and address to what extent the two extra ‘surface’ Au atoms contribute to the electronic structure of the whole cluster, we carried out DFT calculations (see SI for details). In the calculations we adopted a  $[Au_{23}(SCH_3)_{16}]^-$  model cluster mimicking the experimental one by simplifying the  $-SC_6H_{11}$  ligands with  $-SCH_3$ .<sup>44,45</sup> Figure 4A,B shows the experimental and theoretical optical absorption spectra. The theoretical spectrum is convoluted by the Lorentz function with appropriate width. The DFT result reasonably reproduced the spectral profile. The distinct peak at  $\sim 570$  nm in the experimental spectrum corresponds to the simulated peak at  $\sim 530$  nm (with  $\sim 0.16$  eV discrepancy). This peak involves both the HOMO to LUMO (529 nm, intense) and HOMO to LUMO+1 (507 nm, less intense) electronic transitions (Figure 4B).

The diagrams of the HOMO and LUMO of the nanocluster are shown in Figure 4C,D. In the HOMO diagram, we see two large blue lobes of MO clouds. The extra surface Au atoms that serve as the “hubs” indeed contribute to these lobes of MO. The third lobe (red) of the HOMO is located within the cuboctahedron (Figure 4C). In the LUMO diagram (Figure 4D), two blue and two red lobes are seen; the surface “hub” Au atoms are also involved in constructing the electronic state of LUMO. Therefore, the two “hub” atoms are part of the kernel, which give rise to an overall  $Au_{15}$  kernel. It is worth noting that the lowest-lying peak (experiment: 570 nm, theory: 530 nm) in the optical spectrum uniquely arises in the  $Au_{15}$  kernel. Finally, we clarify that the HOMO is not a d-like orbital; instead, it is a hybrid orbital constructed from atomic orbitals of Au. Thus, the  $[Au_{23}(c-C_6)_{16}]^-$  nanocluster is a nonsuperatom, although the nominal valence electron count is 8, being the same as that of superatomic  $[Au_{25}(SR)_{18}]^-$ .<sup>46</sup>

In summary, the  $[Au_{23}(SR)_{16}]^-$  nanocluster exhibits new kernel and surface structures. Unlike the reported  $Au_n(SR)_m$  structures,<sup>20–23,37–39</sup> this nanocluster features a cuboctahedron-based  $Au_{15}$  kernel and  $Au_3(SR)_4$  trimeric staple motifs. Detailed analyses on the geometric and electronic structures offer insight into the nonsuperatomic features of the nanocluster. The experimentally identified new staple motif and kernel structure are remarkable and offer new perspectives in terms of understanding the atomic structure and growth pattern of gold nanoclusters.

## ASSOCIATED CONTENT

### Supporting Information

Details of the synthesis and crystallization, X-ray crystallographic analysis, Figure S1 and S2, and DFT calculations. This material is available free of charge via the Internet at <http://pubs.acs.org>.

## AUTHOR INFORMATION

### Corresponding Authors

rongchao@andrew.cmu.edu  
nobusada@ims.ac.jp

### Notes

The authors declare no competing financial interest.

## ACKNOWLEDGMENTS

K.N. acknowledges research support by Grant-in-Aid (no. 25288012) and by MEXT program “Elements Strategy Initiative to Form Core Research Center” (since 2012) from the Ministry of Education Culture, Sports, Science and Technology (MEXT) of Japan. R.J. thanks research support by the Air Force Office of Scientific Research under AFOSR award no. FA9550-11-1-9999 (FA9550-11-1-0147).

## REFERENCES

- (1) Qian, H.; Zhu, M.; Wu, Z.; Jin, R. *Acc. Chem. Res.* **2012**, *45*, 1470.
- (2) Nishigaki, J.; Tsunoyama, R.; Tsunoyama, H.; Ichikuni, N.; Yamazoe, S.; Negishi, Y.; Ito, M.; Matsuo, T.; Tamao, K.; Tsukuda, T. *J. Am. Chem. Soc.* **2012**, *134*, 14295.
- (3) Qian, H.; Zhu, Y.; Jin, R. *Proc. Natl. Acad. Sci. U.S.A.* **2012**, *109*, 696.
- (4) Shibu, E. S.; Pradeep, T. *Chem. Mater.* **2011**, *23*, 989.
- (5) Dass, A. *J. Am. Chem. Soc.* **2011**, *133*, 19259.
- (6) Knoppe, S.; Azoulay, R.; Dass, A.; Bürgi, T. *J. Am. Chem. Soc.* **2012**, *134*, 20302.
- (7) Yao, H. *J. Phys. Chem. Lett.* **2012**, *3*, 1701.
- (8) Wyrwas, R. B.; Alvarez, M. M.; Khouri, J. T.; Price, R. C.; Schaaff, T. G.; Whetten, R. L. *Eur. Phys. J. D* **2007**, *43*, 91.
- (9) de Silva, N.; Dahl, L. F. *Inorg. Chem.* **2005**, *44*, 9604.
- (10) Shichibu, Y.; Kamei, Y.; Konishi, K. *Chem. Commun.* **2012**, *48*, 7559.
- (11) Wan, X.-K.; Lin, Z.-W.; Wang, Q.-M. *J. Am. Chem. Soc.* **2012**, *134*, 14750.
- (12) Das, A.; Li, T.; Nobusada, K.; Zeng, Q.; Rosi, N. L.; Jin, R. *J. Am. Chem. Soc.* **2012**, *134*, 20286.
- (13) Yang, H.; Wang, Y.; Lei, J.; Shi, L.; Wu, X.; Mäkinen, V.; Lin, S.; Tang, Z.; He, J.; Häkkinen, H.; Zheng, L.; Zheng, N. *J. Am. Chem. Soc.* **2013**, *135*, 9568.
- (14) (a) Liu, Y.; Tsunoyama, H.; Akita, T.; Tsukuda, T. *Chem. Commun.* **2010**, *46*, 550. (b) Li, G.; Jin, R. *Acc. Chem. Res.* **2013**, *46*, 1749.
- (15) Liu, J.; Krishna, K. S.; Losovyj, Y. B.; Chattopadhyay, S.; Lozova, N.; Miller, J. T.; Spivey, J. J.; Kumar, C. S. S. R. *Chem.—Eur. J.* **2013**, *19*, 10201.
- (16) Sexton, J. Z.; Ackerson, C. J. *J. Phys. Chem. C* **2010**, *114*, 16037.
- (17) Wu, Z.; Wang, M.; Yang, J.; Zheng, X.; Cai, W.; Meng, G.; Qian, H.; Wang, H.; Jin, R. *Small* **2012**, *8*, 2027.
- (18) Yau, S. H.; Varnavski, O.; Goodson, T., III. *Acc. Chem. Res.* **2013**, *46*, 1506.
- (19) Devadas, M. S.; Bairu, S.; Qian, H.; Sinn, E.; Jin, R.; Ramakrishna, G. *J. Phys. Chem. Lett.* **2011**, *2*, 2752.
- (20) Jadzinsky, P. D.; Calero, G.; Ackerson, C. J.; Bushnell, D. A.; Kornberg, R. D. *Science* **2007**, *318*, 430.
- (21) Heaven, M. W.; Dass, A.; White, P. S.; Holt, K. M.; Murray, R. W. *J. Am. Chem. Soc.* **2008**, *130*, 3754.
- (22) Zhu, M.; Aikens, C. M.; Hollander, F. J.; Schatz, G. C.; Jin, R. *J. Am. Chem. Soc.* **2008**, *130*, 5883.
- (23) Zhu, M.; Eckenhoff, W. T.; Pintauer, T.; Jin, R. *J. Phys. Chem. C* **2008**, *112*, 14221.
- (24) Pei, Y.; Pal, R.; Liu, C.; Gao, Y.; Zhang, Z.; Zeng, X. C. *J. Am. Chem. Soc.* **2012**, *134*, 3015.
- (25) Jiang, D.-e.; Overbury, S. H.; Dai, S. *J. Am. Chem. Soc.* **2013**, *135*, 8786.
- (26) Malola, S.; Lehtovaara, L.; Knoppe, S.; Hu, K.-J.; Palmer, R. E.; Bürgi, T.; Häkkinen, H. *J. Am. Chem. Soc.* **2012**, *134*, 19560.
- (27) Guidez, E. B.; Aikens, C. M. *J. Phys. Chem. C* **2013**, *117*, 12325.
- (28) Negishi, Y.; Kurashige, W.; Niihori, Y.; Iwasa, T.; Nobusada, K. *Phys. Chem. Chem. Phys.* **2010**, *12*, 6219.
- (29) Qian, H.; Jiang, D.; Li, G.; Gayathri, C.; Das, A.; Gil, R. R.; Jin, R. *J. Am. Chem. Soc.* **2012**, *134*, 16159.
- (30) (a) Shichibu, Y.; Negishi, Y.; Tsunoyama, H.; Kanehara, M.; Teranishi, T.; Tsukuda, T. *Small* **2007**, *3*, 835. (b) Yu, Y.; Luo, Z.; Yu, Y.; Lee, J. Y.; Xie, J. *ACS Nano* **2012**, *6*, 7920.

- (31) Qian, H.; Zhu, Y.; Jin, R. *J. Am. Chem. Soc.* **2010**, *132*, 4583.  
(32) Krommenhoek, P. J.; Wang, J.; Hentz, N.; Johnston-Peck, A. C.; Kozek, K. A.; Kalyuzhny, G.; Tracy, J. B. *ACS Nano* **2012**, *6*, 4903.  
(33) Nimmala, P. R.; Yoon, B.; Whetten, R. L.; Landman, U.; Dass, A. *J. Phys. Chem. A* **2013**, *117*, 504.  
(34) Qian, H.; Jin, R. *Chem. Mater.* **2011**, *23*, 2209.  
(35) Negishi, Y.; Sakamoto, C.; Ohyama, T.; Tsukuda, T. *J. Phys. Chem. Lett.* **2012**, *3*, 1624.  
(36) Tang, Z.; Robinson, D. A.; Bokossa, N.; Xu, B.; Wang, S.; Wang, G. *J. Am. Chem. Soc.* **2011**, *133*, 16037.  
(37) Zeng, C.; Li, T.; Das, A.; Rosi, N. L.; Jin, R. *J. Am. Chem. Soc.* **2013**, *135*, 10011.  
(38) Zeng, C.; Qian, H.; Li, T.; Li, G.; Rosi, N. L.; Yoon, B.; Barnett, R. N.; Whetten, R. L.; Landman, U.; Jin, R. *Angew. Chem., Int. Ed.* **2012**, *51*, 13114.  
(39) Qian, H.; Eckenhoff, W. T.; Zhu, Y.; Pintauer, T.; Jin, R. *J. Am. Chem. Soc.* **2010**, *132*, 8280.  
(40) Pei, Y.; Gao, Y.; Shao, N.; Zeng, X. C. *J. Am. Chem. Soc.* **2009**, *131*, 13619.  
(41) Jiang, D.-e.; Chen, W.; Whetten, R. L.; Chen, Z. *J. Phys. Chem. C* **2009**, *113*, 16983.  
(42) Zhu, M.; Qian, H.; Jin, R. *J. Am. Chem. Soc.* **2009**, *131*, 7220.  
(43) Tlahuice, A.; Garzon, I. L. *Phys. Chem. Chem. Phys.* **2012**, *14*, 3737.  
(44) Iwasa, T.; Nobusada, K. *J. Phys. Chem. C* **2007**, *111*, 45.  
(45) Nobusada, K. *J. Phys. Chem. B* **2004**, *108*, 11904.  
(46) Akola, J.; Walter, M.; Whetten, R. L.; Hakkinen, H.; Gronbeck, H. *J. Am. Chem. Soc.* **2008**, *130*, 3756.